RSC Advances

ROYAL SOCIETY OF CHEMISTRY

www.rsc.org/advances

Journal Name

ARTICLE

Band gap engineering of graphenylene by hydrogenation and halogenation: a density functional theory study

Received 00th January 20xx,
Accepted 00th January 20xx

DOI: 10.1039/x0xx00000x

www.rsc.org/

Wei Liu,[a] Mao-sheng Miao,[bc] and Jing-yao Liu[*a]

Graphenylene, a new form of two-dimensional (2D) carbon allotrope consisting of non-delocalized sp^2-carbon atoms, has aroused considerable interest recently due to its thermodynamic stability and porous structure. In this work, density functional theory is used to investigate the hydrogenation and halogenation of graphenylene. The adsorption stability of hydrogen and halogen atoms on graphenylene is discussed at different concentrations of adsorbate atoms. The electronic structures of functionalized graphenylenes show that by controlling the concentration of adsorbate atoms, the band gap of graphenylene could be tuned in a wide range, from 0.075 to 4.98 eV by hydrogenation and 0.024 eV to 4.87 eV by halogenation.

1. Introduction

Graphene, an atomic monolayer of graphite consisting of sp^2 carbon atoms that are arranged in a honeycomb lattice,[1] is a promising 2D material for applications in many emerging technologies.[2,3] It has attracted tremendous attention in the last decade because of its peculiar electronic and physical properties, such as the Dirac cone structure, exceptional carrier mobility,[4–6] high thermal conductivity[7] and high mechanical strength.[8,9] However, graphene is intrinsically metallic with zero-gap, which hinders its application in 2D based electronic devices. Therefore, much effort has been devoted to engineer its band gap. Chemical functionalization is an effective way to modify the electronic properties of graphene. Recent researches have demonstrated that hydrogenation and fluorination can tune the band gap of graphene up to ~ 5.4 and ~ 7.0 eV respectively,[10–15] for example, Gao et al.[15] theoretically predicted that the band gap of hydrogenated graphene with paired hydrogen vacancies can be tailored continuously from 0 to 4.66 eV, depending on hydrogen coverage and configurations. But this tuning has limitation, since hydrogen or fluorine atoms adsorbed on graphene were found to tend to aggregate with each other in experiments. Recent experimental studies showed that the functionalization level of graphene can be precisely controlled by using a reactive ion etching plasma[16] or the scanning probe technique.[17] These experimental evidences will lead to the development of graphene-based electronic devices.

On the other hand, it is well known that carbon atoms have the ability to exist in different hybridizations. Thus, searching new forms of 2D carbon allotropes has aroused considerable interest from both academe and industry. Many of carbon allotropes such as graphyne and graphdiyne have been predicted to have unique electronic and mechanical properties.[18,19] Graphenylene, a new full sp^2-hybridized carbon network, possesses the same point group, D_{6h}, as graphene. The structure, consisting of hexatomic and tetratomic rings with porous structures, was firstly proposed by Balaban[20] and the properties have been investigated.[21–23] In one recent paper, Zhi et al[24] studied the structural and electronic properties of graphenylene by first-principles calculation. They predicted that graphenylene is a true minimum on the potential energy surface and the first example of a non-delocalized sp^2-carbon structure. More specifically, graphenylene is predicted to be a semiconductor with a narrow direct band gap of 0.025 eV. In addition, ab initio quantum molecular dynamics calculation[25] showed that graphenylene could be formed by selective dehydrogenation of porous graphene, which implies that the possibility of the synthesis of graphenylene.

Lee et al[26–28] recently reported the first-principles studies on tailoring the band gaps of two carbon allotropes, graphyne and graphdiyne, by hydrogenation and halogenation. Their calculations showed that different from the case occurring on

[a] Institute of Theoretical Chemistry, Jilin University, Changchun, P. R. China
[b] Department of Chemistry and Biochemistry, California State University Northridge, CA, USA
[c] Beijing Computational Science Research Center, Beijing, P. R. China

† Electronic Supplementary Information (ESI) available: [The structures of halogenated graphenylene in one unit cell and the calculated PBE energies of the obtained functionalized graphenylene]. See DOI: 10.1039/x0xx00000x

graphene, hydrogen or halogen atoms preferentially adsorb on carbon atoms with no clustering. Therefore, it is natural to inquire whether the band gap of graphenylene can also be modified by hydrogenation and halogenation, and what sizable band gap can be opened. Considering the unique electronic and structural properties as well as the potential applications in semiconductor-based electronic devices and energy storage,[29] in the present work, we performed a systematic density functional theory (DFT) study to investigate the hydrogenation and halogenation of graphenylene. The geometrical and electronic properties of hydrogenated and halogenated graphenylenes were obtained. The change of band gaps of functionalized graphenylenes depending on the type and the concentrations of adsorbates is discussed. The results show that by controlling the concentration of adsorbate atoms, the band gap of graphenylene could be tuned up to 4.98 eV by hydrogenation and 4.87 eV by halogenation, comparable to band gap tuning of 4.5 (3.04) and 3.0 (5.20) eV by hydrogenation and halogenation of graphyne[26,28] (graphdiyne[27]). The analysis of the absolute energies of the edge states of functionalized graphenylenes demonstrates that they may have application potentials in photocatalysis. Our aim is to provide a comprehensive understanding for the implications of graphenylene for potential 2D device applications based on the predicted tunable band gap trend.

2. Methodology

All the first-principles calculations were performed based on periodic density functional theory using Vienna Ab-Initio Simulation Package (VASP)[30] with a projector augmented wave (PAW)[31] approach. The electron exchange and correlation were treated by the generalized gradient approximation (GGA) with Perdew-Burke-Ernzerhof (PBE)[32] functional. Neighboring slabs are separated by a vacuum region of about 20 Å along the z-direction to avoid interactions between them. Monkhorst-Pack[33] $8 \times 8 \times 1$ k-point mesh was used for structure optimizations. The cutoff energy in the plane-wave expansion was set to 900 eV. To obtain accurate band gap values, Heyd-Scuseria-Ernzerhof (HSE)[34] hybrid functional was also used to calculate the band structures.

3. Results and discussion

Graphenylene is composed of cyclohexatriene units with 12 carbon atoms in one unit cell. The optimized structure of graphenylene in a 2×2 supercell is shown in Fig. 1a. The calculated lattice parameters of graphenylene are a = b = 6.764 Å. In one hexatomic ring of graphenylene there are two different C-C bonds, one C-C double bond and one C-C single bond. Adding the C-C single bond between two neighboring hexatomic rings, there are totally three different C-C bonds in graphenylene. The bond length of the double bond is 1.366 Å and the bond lengths of the other two single bonds are 1.471 and 1.479 Å, respectively. All these obtained geometrical parameters are in good agreement with previous results.[24] In present work, we study both hydrogenated and halogenated graphenylene, CM_x, where M presents hydrogen or halogen (fluorine, chlorine, bromine and iodine) atoms, and x is the concentration of the adsorbates. For the hydrogenation and halogenation of graphenylene, the hydrogen or halogen atoms can bind to each sp^2 carbon atom of one double bond with one atom above the graphenylene plane and the other below the plane. There are totally six double bonds in one graphenylene unit cell, thus the concentration of the adsorbate atoms x equals to 0.17, 0.33, 0.50, 0.67, 0.83 and 1.00.

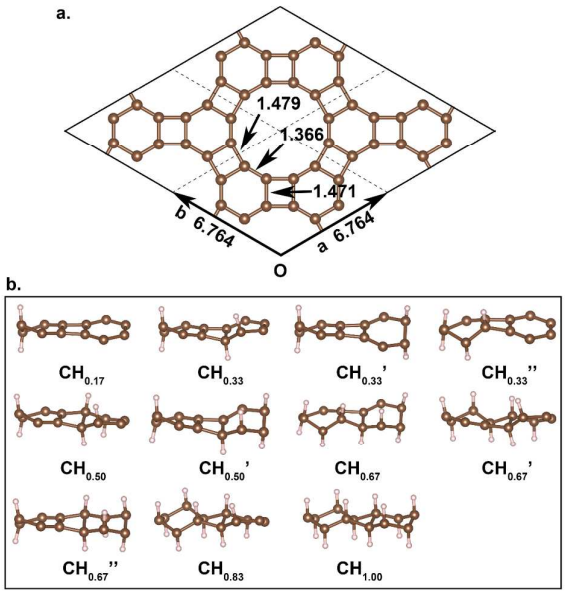

Figure 1. (a) Two dimensional structure of pristine graphenylene in a 2×2 supercell. The unit of lattice parameters and bond lengths is angstrom. (b) The structures of hydrogenated graphenylene in one unit cell at various

The optimized structures of hydrogenated graphenylenes in one unit cell at various concentrations are shown in Fig. 1. The six double bonds in one graphenylene unit cell are identical, thus at x = 0.17, 0.83 and 1.00 the structures of hydrogenated graphenylenes are unique, while there are three, two and three kinds of structures (labeled by apostrophe) at the concentrations of 0.33, 0.50 and 0.67, respectively, based on the different adsorption sites of hydrogen atoms. Through hydrogenation, the hybridization of carbon atoms is changed from sp^2 to sp^3. The structures vary from strictly two dimensional to corrugate gradually with the increase of the hydrogen concentration. In $CH_{1.00}$, both the two hexatomic rings are in chair conformation. The in plane lattice constant of graphenylene was decreased by 0.040, 0.125 and 0.009 Å at x = 0.17, 0.33 and 0.67 respectively, while it was increased by 0.013, 0.120 and 0.176 Å at x = 0.50, 0.83 and 1.00, respectively. Lattice constants a and b are always equivalent at each concentration. The structures of halogenated graphenylenes are studied similarly. Through calculation we found that if the concentration x and the locations of adsorbate atoms are the same, the optimized structures of halogenated graphenylenes are almost the same as hydrogenated graphenylenes, except that the C-M bond lengths increase as the atomic number increases from hydrogen to iodine. For example, the calculated C-M bond lengths in $CM_{0.17}$ are 1.102, 1.402, 1.812, 2.000 and 2.224 Å for C-H, C-F, C-Cl, C-Br and C-I bonds respectively. The lattice constants of halogenated graphenylenes decrease at lower concentrations, x = 0.17 and 0.33, while increase at higher concentrations x = 0.50 ~ 1.00. The optimized structures of halogenated graphenylenes and the lattice constants of functionalized graphenylenes are shown in Supporting Information. In the following sections, only the most stable structures of hydrogenated and halogenated graphenylenes at each concentration are further studied to understand the thermodynamic and electronic properties of chemically functionalized graphenylenes.

The binding energy of per adsorbate atom in CM_x is defined as

$$E^{x}_{binding}(\mathrm{M}) = (E_{CM_x} - E_{graphenylene} - n \cdot E_M)/n$$

where E_{CM_x} is the total energy of functionalized graphenylene CM_x, $E_{\mathrm{graphenylene}}$ is the total energy of pristine graphenylene, E_M is the energy per M atom of an M_2 molecule in vacuum, and n is the number of adsorbed M atoms per unit cell for a given x. The calculated binding energies as a function of the concentration x are presented in Fig. 2. Seen from Fig. 2, the binding of fluorine to graphenylene is always the most stable at each concentration, which can be attributed to the strongest electronegativity and small ionic radius of fluorine. For example, the calculated binding energies are -0.45, -2.21, -0.50 and -0.18 eV/atom for H, F, Cl and Br, respectively, at x = 0.17. As the concentration x increases, the binding energies of

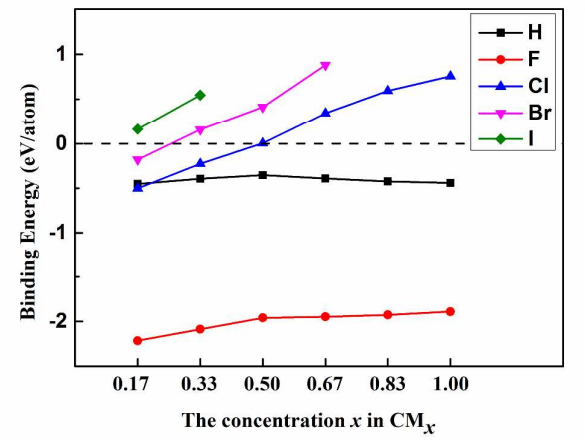

Figure 2. The binding energies of hydrogen and halogen atoms as a function of the concentration x.

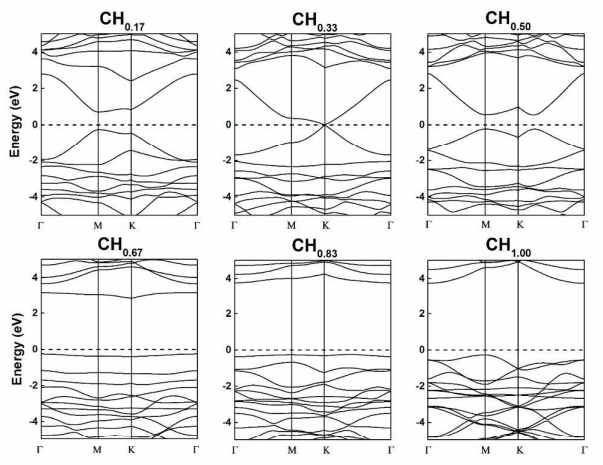

Figure 3. The PBE band structures of hydrogenated graphenylenes at different hydrogen concentration x. The Fermi levels are shown by dashed lines.

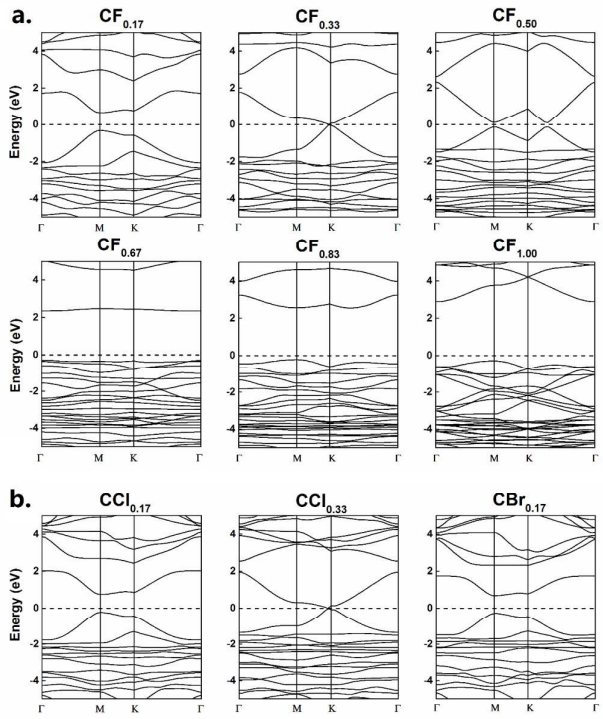

Figure 4. (a) The PBE band structures of fluorinated graphenylenes at different fluorine concentration x. (b) The PBE band structures of halogenated graphenylenes $CCl_{0.17}$, $CCl_{0.33}$ and $CBr_{0.17}$. The Fermi levels are shown by dashed lines.

hydrogen are nearly unchanged and the binding energies of fluorine slightly increase, while the changes in the binding energies of chlorine and bromine atoms are much larger. It is seen that the adsorption processes become endothermic when the concentration x of chlorine and bromine is larger than 0.33 and 0.17, respectively, and for iodine, the calculated binding energies at any concentration are all positive, indicating that the adsorption of Cl, Br and I at these concentrations is unstable. In addition, the change trend of these binding energies as a function of the concentration x in Fig. 3 indicates the repulsive interaction between adsorbate atoms (hydrogen/halogen atoms). As a result, the clustering of hydrogen and halogen atoms is energetically unfavorable on graphenylene, making band gap tunable by hydrogenation and halogenation. The adsorption structure features of hydrogenated and halogenated graphenylenes are very similar to previous studies on functionalized graphyne and graphdiyne.[26,27]

The electronic properties of hydrogenated and halogenated graphenylenes are studied. The PBE band gap of pristine graphenylene was calculated to be 0.039 eV, which is in good agreement with the previously reported value 0.025 eV.[24] The PBE band structures of hydrogenated graphenylenes at different hydrogen concentrations are presented along the high symmetry lines of the Brillouin zone in Fig. 3. At

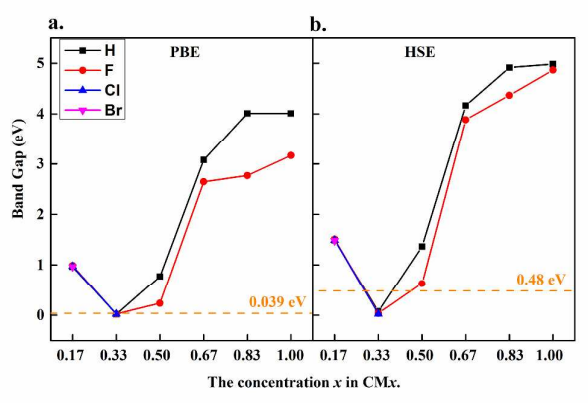

Figure 5. The calculated PBE (a) and HSE (b) band gap values of functionalized graphenylenes as a function of the concentration x. The orange dashed lines and numbers indicate the band gap values of pristine graphenylene.

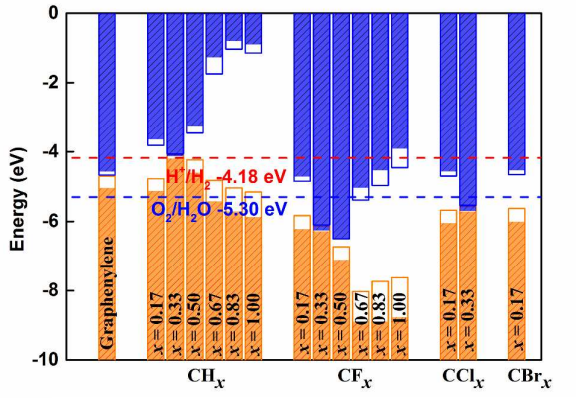

Figure 6. Band edges of graphenylene and functionalized graphenylenes relative to the vacuum level. The blue and brown lines represent the PBE results, while the columns filled by blue and brown colors represent the HSE results. The dashed lines indicate the water redox potentials.

concentrations of x = 0.17, 0.33 and 0.50, the stable hydrogenated graphenylenes have direct band gaps of 0.96, 0.021 and 0.77 eV, with the valence band maximum (VBM) and conduction band minimum (CBM) located at the M point, K point and between K and Γ, respectively; while at x = 0.67, 0.83 and 1.00, three indirect band gaps of 3.08, 4.01 and 4.01 eV, respectively, are obtained. In the band structures of $CH_{0.17}$, $CH_{0.33}$ and $CH_{0.50}$, the bands around both VBM and CBM exhibit very large dispersion, indicating higher mobilities of both electrons and holes; on the contrary, at higher concentrations (x > 0.50), the bands of VBM and CBM become much flatter, implying these hydrogenated graphenylenes may have lower mobilities of both electrons and holes.

In Fig. 4a, the band structures of fluorinated graphenylenes are illustrated. It is shown that the characteristics of these band structures are very similar with that of hydrogenated graphenylenes. At x = 0.17 and 0.33, two semiconductors with direct gaps of 0.99 and 0.024 eV, respectively, are obtained. The VBM and CBM positions of $CF_{0.17}$ are located at the M point, while those of $CF_{0.33}$ are located to the left of the K point. $CF_{0.50}$ is a semiconductor with an indirect gap of 0.24 eV. Its VBM is located at the M point and its CBM is located between the K and Γ point. At higher concentrations (x > 0.5), the band gaps of fluorinated graphenylenes are calculated to be 2.65, 2.77 and 3.17 eV. As the case in hydrogenated graphenylenes, the mobilities of electrons and holes of fluorinated graphenylenes may be higher at the F concentrations from x = 0.17 to 0.50, while much lower at x = 0.67, 0.83 and 1.00. In Fig. 4b, the band structures of $CCl_{0.17}$, $CCl_{0.33}$ and $CBr_{0.17}$ are illustrated. Clearly, the band structures of CCl_x and CBr_x show similar features with those of CF_x. They are predicted to be semiconductors with direct band gaps of 0.98, 0.026 and 0.97 eV, respectively.

The calculated PBE band gaps of hydrogenated and halogenated graphenylenes as a function of the concentration x are presented In Fig. 5a. Since the local and semilocal functionals such as PBE functional are known to underestimate the band gaps, and hybrid DFT functionals such as HSE in general describe quite accurate band gaps when compared with the experimental values.[34] Therefore, HSE functional is also employed to predict the band gaps of functionalized graphenylenes. The HSE band gaps of hydrogenated and halogenated graphenylenes are shown in Fig. 5b. The HSE band gap of graphenylene is 0.48 eV, thus the band gap of pristine graphenylene is underestimated by 0.44 eV using the PBE. From Fig. 5a-b, it is seen that the functionalized graphenylenes exhibit a wide band gap semiconducting behavior and both PBE and HSE gaps change in the similar trend as a function of the concentrations. At the x = 0.17 concentration, the band gap is enlarged compared to that of pristine graphenylene, while it decreases to a much narrow gap at x = 0.33. As the concentration x increases from x = 0.33 to 1.00, the band gaps increase and the gap values of hydrogenated graphenylenes are larger than those of fluorinated graphenylenes. For example, at x = 0.50, the HSE band gap of hydrogenated graphenylene is 1.37 eV, which is 0.74 eV larger than that of fluorinated graphenylene.

Therefore, one can find that the band gap of graphenylene can be tuned in a wide range, 0.075 to 4.98 eV by hydrogenation and 0.024 eV to 4.87 eV by halogenation.

At last, the absolute energies of the edge states of hydrogenated and halogenated graphenylenes at various concentrations are studied, because the VBM and CBM positions are important for the application of 2D material as photocatalyst for water splitting and organic pollutants degradation. By aligning the average electrostatic potentials of the 2D sheets with that of the vacuum, the VBM and CBM positions calculated by both HSE and PBE are plotted in Fig. 6. Note that at the x = 0.17 and 0.33 concentrations, the band edge positions of fluorinated graphenylenes are very close to those of chlorinated and brominated graphenylenes, while quite different from those of hydrogenated graphenylenes, although their band gaps are almost the same. Generally speaking, both CBM and VBM energies of fluorinated (or halogenated) graphenylenes are lower than those of hydrogenated graphenylenes, which means that fluorinated graphenylenes possess larger ionization energies and electron affinities. As an example, the redox potentials of water[35] are also given in the figure. It is seen that the band edges of $CH_{0.67}$, $CH_{0.83}$, $CH_{1.00}$ and $CF_{1.00}$ satisfy the band edge requirement, straddling well with the water redox potentials as shown in Fig. 6. As a consequence, the reduction and oxidation processes of water are thermodynamically favorable. For $CH_{0.67}$, $CH_{0.83}$, $CH_{1.00}$ and $CF_{1.00}$, their CBM are 2.91, 3.38, 3.29 and 0.26 eV more positive than the reduction potential of H^+/H_2, and their VBM are 0.13, 0.41, 0.57 and 3.48 eV more negative than the oxidation level of O_2/H_2O. It is seen that $CH_{0.83}$ has the largest energy difference between CBM and the reduction potential of H^+/H_2 and $CF_{1.00}$ has the largest energy difference between VBM and the oxidation potential of O_2/H_2O. As stated in previous papers,[36,37] the larger energy difference between CBM/VBM and the water reduction/oxidation potential, the higher the reducing/oxidizing power. Therefore, $CH_{0.83}$ and $CF_{1.00}$ possess the strongest reducing and oxidizing capability respectively. For the rest obtained functionalized graphenylenes, $CH_{0.17}$ and $CH_{0.50}$ have favorable CBM positions for hydrogen production, while $CF_{0.17}$, $CF_{0.67}$, $CF_{0.83}$, $CCl_{0.17}$ and $CBr_{0.17}$ possess good enough VBM positions for oxygen production. Above all discussions, the functionalized graphenylenes may have application potentials in catalysis.

4. Conclusions

In this work, the hydrogenation and halogenation of graphenylene are studied using first-principles calculations. Hydrogen and fluorine atoms preferentially bind to graphenylene to form sp^3 hybridized bonds at all the concentrations considered, the adsorption of chlorine and bromine is favorable only at lower concentrations, while iodine atoms are unstable at any concentrations. The change trend of the calculated binding energies indicated the clustering of hydrogen and halogen atoms on graphenylene is not preferable, which makes band gap tunable by hydrogenation and halogenation. The electronic structures of functionalized graphenylenes at different concentrations of adsorbate atoms show that hydrogenated and halogenated graphenylenes exhibit a wide band gap semiconducting behavior. By controlling the type and concentration of adsorbate atoms, the band gap of graphenylene can be tuned in a wide range, 0.075 to 4.98 eV by hydrogenation and 0.024 eV to 4.87 eV by halogenation. Our present study may be useful for broadening the potential applications of functionalized graphenylenes in nanoelectronics.

Acknowledgements

This research was supported by the National Natural Science Foundation of China (Grants No. 21373098).

References

1 K. S. Novoselov, A. K. Geim, S. V. Morozov, D. Jiang, Y. Zhang, S. V. Dubonos, I. V. Grigorieva and A. A. Firsov, *Science*, 2004, **306**, 666–669.
2 A. K. Geim and K. S. Novoselov, *Nat. Mater.*, 2007, **6**, 183–191.
3 A. K. Geim, *Science*, 2009, **324**, 1530–1534.
4 A. S. Mayorov, R. V. Gorbachev, S. V. Morozov, L. Britnell, R. Jalil, L. A. Ponomarenko, P. Blake, K. S. Novoselov, K. Watanabe, T. Taniguchi and A. K. Geim, *Nano Lett.*, 2011, **11**, 2396–2399.
5 K. S. Novoselov, A. K. Geim, S. V. Morozov, D. Jiang, M. I. Katsnelson, I. V. Grigorieva, S. V. Dubonos and A. A. Firsov, *Nature*, 2005, **438**, 197–200.
6 S. V. Morozov, K. S. Novoselov, M. I. Katsnelson, F. Schedin, D. C. Elias, J. A. Jaszczak and A. K. Geim, *Phys. Rev. Lett.*, 2008, **100**, 016602.
7 A. A. Balandin, *Nat. Mater.*, 2011, **10**, 569–581.
8 C. Lee, X. Wei, J. W. Kysar and J. Hone, *Science*, 2008, **321**, 385–388.
9 F. Liu, P. Ming and J. Li, *Phys. Rev. B*, 2007, **76**, 064120.
10 P. Cudazzo, C. Attaccalite, I. V. Tokatly and A. Rubio, *Phys. Rev. Lett.*, 2010, **104**, 226804.
11 R. Balog, B. Jørgensen, L. Nilsson, M. Andersen, E. Rienks, M. Bianchi, M. Fanetti, E. Lægsgaard, A. Baraldi, S. Lizzit, Z. Sljivancanin, F. Besenbacher, B. Hammer, T. G. Pedersen, P. Hofmann and L. Hornekær, *Nat. Mater.*, 2010, **9**, 315–319.
12 O. Leenaerts, H. Peelaers, A. D. Hernández-Nieves, B. Partoens and F. M. Peeters, *Phys. Rev. B*, 2010, **82**, 195436.
13 W. Wei and T. Jacob, *Phys. Rev. B*, 2013, **87**, 115431.
14 K.-J. Jeon, Z. Lee, E. Pollak, L. Moreschini, A. Bostwick, C.-M. Park, R. Mendelsberg, V. Radmilovic, R. Kostecki, T. J. Richardson and E. Rotenberg, *ACS Nano*, 2011, **5**, 1042–1046.
15 H. Gao, L. Wang, J. Zhao, F. Ding and J. Lu, *J. Phys. Chem. C*, 2011, **115**, 3236–3242.
16 M. Wojtaszek, N. Tombros, A. Caretta, P. H. M. van Loosdrecht and B. J. van Wees, *J. Appl. Phys.*, 2011, **110**, 063715.
17 I.-S. Byun, W. Kim, D. W. Boukhvalov, I. Hwang, J. W. Son, G. Oh, J. S. Choi, D. Yoon, H. Cheong, J. Baik, H.-J. Shin, H. W. Shiu, C.-H. Chen, Y.-W. Son and B. H. Park, *NPG Asia Mater.*, 2014, **6**, e102.
18 D. Malko, C. Neiss, F. Viñes and A. Görling, *Phys. Rev. Lett.*, 2012, **108**, 086804.
19 X. Niu, X. Mao, D. Yang, Z. Zhang, M. Si and D. Xue, *Nanoscale Res. Lett.*, 2013, **8**, 469.
20 A. T. Balaban, C. C. Rentea and E. Ciupitu, *Rev Roum Chim*, 1968, **13**, 231–247.

21 A. T. Balaban, *Comput. Math. Appl.*, 1989, **17**, 397–416.
22 H. Zhu, A. T. Balaban, D. J. Klein and T. P. Živković, *J. Chem. Phys.*, 1994, **101**, 5281–5292.
23 A. T. Balaban, D. J. Klein and C. A. Folden, *Chem. Phys. Lett.*, 1994, **217**, 266–270.
24 Q. Song, B. Wang, K. Deng, X. Feng, M. Wagner, J. D. Gale, K. Müllen and L. Zhi, *J. Mater. Chem. C*, 2012, **1**, 38–41.
25 G. Brunetto, P. A. S. Autreto, L. D. Machado, B. I. Santos, R. P. B. dos Santos and D. S. Galvão, *J. Phys. Chem. C*, 2012, **116**, 12810–12813.
26 J. Koo, B. Huang, H. Lee, G. Kim, J. Nam, Y. Kwon and H. Lee, *J. Phys. Chem. C*, 2014, **118**, 2463–2468.
27 J. Koo, M. Park, S. Hwang, B. Huang, B. Jang, Y. Kwon and H. Lee, *Phys. Chem. Chem. Phys.*, 2014, **16**, 8935–8939.
28 J. Koo, H. J. Hwang, B. Huang, H. Lee, H. Lee, M. Park, Y. Kwon, S.-H. Wei and H. Lee, *J. Phys. Chem. C*, 2013, **117**, 11960–11967.
29 Y.-X. Yu, *J. Mater. Chem. A*, 2013, **1**, 13559–13566.
30 G. Kresse and J. Furthmüller, *Phys. Rev. B*, 1996, **54**, 11169–11186.
31 P. E. Blöchl, *Phys. Rev. B*, 1994, **50**, 17953–17979.
32 J. P. Perdew, K. Burke and M. Ernzerhof, *Phys. Rev. Lett.*, 1996, **77**, 3865–3868.
33 H. J. Monkhorst and J. D. Pack, *Phys. Rev. B*, 1976, **13**, 5188–5192.
34 J. Heyd, G. E. Scuseria and M. Ernzerhof, *J. Chem. Phys.*, 2003, **118**, 8207–8215.
35 X. Wang, K. Maeda, A. Thomas, K. Takanabe, G. Xin, J. M. Carlsson, K. Domen and M. Antonietti, *Nat. Mater.*, 2009, **8**, 76–80.
36 X. Jiang, J. Nisar, B. Pathak, J. Zhao and R. Ahuja, *J. Catal.*, 2013, **299**, 204–209.
37 X. Jiang, P. Wang and J. Zhao, *J. Mater. Chem. A*, 2015, **3**, 7750–7758.